Global Sensing and Its Impact for Quantum Many-Body Probes with Criticality

Victor Montenegro,* Utkarsh Mishra,† and Abolfazl Bayat‡
Institute of Fundamental and Frontier Sciences, University of Electronic Science and Technology of China, Chengdu 610051, China

(Received 11 February 2021; accepted 13 April 2021; published 17 May 2021)

Quantum sensing is one of the key areas that exemplify the superiority of quantum technologies. Nonetheless, most quantum sensing protocols operate efficiently only when the unknown parameters vary within a very narrow region, i.e., local sensing. Here, we provide a systematic formulation for quantifying the precision of a probe for multiparameter global sensing when there is no prior information about the parameters. In many-body probes, in which extra tunable parameters exist, our protocol can tune the performance for harnessing the quantum criticality over arbitrarily large sensing intervals. For the single-parameter sensing, our protocol optimizes a control field such that an Ising probe is tuned to always operate around its criticality. This significantly enhances the performance of the probe even when the interval of interest is so large that the precision is bounded by the standard limit. For the multiparameter case, our protocol optimizes the control fields such that the probe operates at the most efficient point along its critical line. Finally, it is shown that even a simple magnetization measurement significantly benefits from our global sensing protocol.

DOI: 10.1103/PhysRevLett.126.200501

Introduction.—The emerging field of quantum sensing exploits quantum features for developing a new class of sensors with unprecedented precision [1–6]. Originally, the superiority of quantum sensors was shown by exploiting the quantum superposition of Greenberger-Horne-Zeilinger–type states in noninteracting particles [7–10]. Such sensors use the resources (e.g., the number of particles L) more efficiently to enhance their precision, quantified by the variance of the estimation, from the usual classical standard limit (bounded by $1/L$) to the Heisenberg limit (bounded by $1/L^2$) [11,12]. However, if the particles interact, the precision goes down [13–16]. Moreover, the Greenberger-Horne-Zeilinger states are difficult to create and prone to decoherence [17–22]. Hence, developing these types of sensors for many particles, where the quantum enhancement becomes significant, is extremely challenging in practice. To overcome such difficulties, a plethora of novel methods and systems have been exploited for sensing purposes, including quantum control techniques [23–26], machine learning algorithms [27–29], hybrid variational methods [30], feedback schemes [31–34], quantum chaos [35], periodically driven systems [36,37], and sequential measurements [38–41].

Strongly correlated many-body systems are among the efficient quantum probes [42–48]. In particular, the ground state of many-body systems with quantum phase transitions is known to provide quantum-enhanced sensing at the vicinity of their critical point [49–58]. These schemes truly exploit the interaction between the particles, and, because of operation at equilibrium, they benefit from easier preparation and robustness against decoherence. However, the quantum-enhanced sensing only occurs at the vicinity of the critical point [49], making these sensors most suitable for local sensing, where the unknown parameter varies within a very narrow interval. Hence, tuning the system to operate optimally at its quantum phase transition point can be very elusive and practically demanding, e.g., adaptive sensing strategies have to be employed [2,59–66]. A key open question is whether one can employ such sensors for global sensing, where the unknown parameter varies over a wide range. While in the case of temperature there have been efforts for the formulation of global thermometry [67,68], the problem is still open for general quantum sensing.

In this Letter, we formulate a systematic approach for multiparameter global sensing, where the unknown parameters can vary over arbitrarily large intervals. Our protocol applies to any sensing protocol and provides a systematic approach for optimizing the probe. In particular, for many-body sensors, we show that one can genuinely exploit the criticality as a resource for enhancing the global multidirectional magnetometry precision.

Parameter estimation.—Every sensing protocol contains three essential steps: (i) choose an appropriate probe, (ii) gather data through repeatedly performing specific types of measurements on the probe, and (iii) feed the gathered data into an estimator to infer the value of the unknown parameters. The precision of the estimation of an unknown parameter $\boldsymbol{h} = (h_1, h_2, \ldots)$ obeys the Cramér-Rao inequality [69,70]

$$\mathrm{Cov}(\boldsymbol{h}) \geq M^{-1}\mathcal{F}_C(\boldsymbol{h})^{-1} \geq M^{-1}\mathcal{F}_Q(\boldsymbol{h})^{-1}, \qquad (1)$$

where $\mathrm{Cov}(\boldsymbol{h})$ is the covariance matrix whose elements are $[\mathrm{Cov}(\boldsymbol{h})]_{\mu,\nu} = \langle h_\mu h_\nu\rangle - \langle h_\mu\rangle\langle h_\nu\rangle$, M is the total number of measurements, and $\mathcal{F}_C(\boldsymbol{h})$ and $\mathcal{F}_Q(\boldsymbol{h})$ are the classical and quantum Fisher information (QFI) matrices, respectively [71]. For a given quantum probe with density matrix $\rho(\boldsymbol{h})$ and a specific positive operator-valued measure (POVM) $\{\Pi_k\}$, the bound is given by the classical Fisher information matrix $[\mathcal{F}_C(\boldsymbol{h})]_{\mu,\nu} = \sum_k p_k(\boldsymbol{h})[\partial_\mu \log p_k(\boldsymbol{h})][\partial_\nu \log p_k(\boldsymbol{h})]$, where $p_k(\boldsymbol{h}) = \mathrm{Tr}[\rho(\boldsymbol{h})\Pi_k]$ is the probability of measurement outcome k, and $\partial_\nu := \partial/\partial h_\nu$. By optimizing over all possible POVMs, one can tighten the bound to be given by the QFI $\mathcal{F}_Q(\boldsymbol{h})$ [70,71], which can be simplified for pure states $\rho(\boldsymbol{h}) = |\Phi(\boldsymbol{h})\rangle\langle\Phi(\boldsymbol{h})|$ as $[\mathcal{F}_Q(\boldsymbol{h})]_{\mu,\nu} = 4\mathrm{Re}[\langle\partial_\mu\Phi|\partial_\nu\Phi\rangle - \langle\Phi|\partial_\mu\Phi\rangle\langle\Phi|\partial_\nu\Phi\rangle]$ [72]. In the case of single parameter, Eq. (1) reduces to

$$\delta h^2 \geq M^{-1}\mathcal{F}_Q(h)^{-1}, \tag{2}$$

in which the QFI provides the ultimate bound for the variance of the estimation. Note that, for any given probe one can indeed saturate the inequality of Eq. (2) by using an appropriate measurement setup computed through symmetric logarithmic derivatives [71,73,74] and an optimal estimator (which for a large dataset is known to be Bayesian [75–79]). However, the optimal measurement basis, in general, depends on the unknown parameter h, which varies over an interval $[h^{\min}, h^{\max}]$. The optimal sensing is thus applicable only when $\Delta h = h^{\max} - h^{\min}$ is small, which is called *local* sensing. In this situation, the optimal measurement can be chosen for $h^{\mathrm{cen}} = (h^{\max} + h^{\min})/2$. For large Δh, the criteria for the best sensing protocol is indeed unknown. The situation for multiparameter estimation is more complex as, due to the noncommutativity of the optimal POVMs for different parameters, even for local sensing the Cramér-Rao bound may not be achievable [74].

Single-parameter global sensing.—In the case of local sensing (i.e., small Δh), the Cramér-Rao bound in Eq. (2) can always be saturated. Nonetheless, the sensing procedure might still be highly suboptimal due to the bad choice of the probe. Hence, an optimal local sensing algorithm requires optimization of $\mathcal{F}_Q(h^{\mathrm{cen}})$ with respect to the parameters of the probe. For large Δh, which is called *global* sensing, the situation is more complex as (i) in general the optimal measurement basis varies over Δh and no measurement setup can saturate the Cramér-Rao bound over the entire interval, and (ii) it is not clear which quantity has to be optimized to find the optimal probe. In the following, we address this problem.

To formulate the global sensing, we first quantify the average uncertainty of the estimation via $\int_{\Delta h}\delta h^2 f(h)dh$, where $f(h)$ is the prior information, i.e., the probability distribution, of the unknown parameter h over the sensing interval Δh of interest. Note that every practical sensor has a range of functionality, which might be different from Δh. In general, the functionality range of the probe needs to be larger than Δh. From Eq. (2), one can easily show that this average uncertainty is bounded by

$$g(\boldsymbol{B}) := \int_{\Delta h}\frac{f(h)}{M\mathcal{F}_Q(h|\boldsymbol{B})}dh, \tag{3}$$

where $\boldsymbol{B} = (B_1, B_2, \ldots)$ are external tunable parameters interacting with the probe. We define the minimization of $g(\boldsymbol{B})$ with respect to control parameters $\boldsymbol{B}$ as a figure of merit for finding the optimal probe, namely $g(\boldsymbol{B}^*) := \min_{\boldsymbol{B}}[g(\boldsymbol{B})]$. For the minimization of $g(\boldsymbol{B})$, if the number of parameters are few, such as the case in this Letter, one can adopt a brute-force search method. Otherwise, other optimization algorithms such as the gradient-based Newton-Raphson method [80] or gradient-free genetic algorithms [81] can be exploited. Throughout this Letter, we assume no prior information about the unknown parameter h, and thus $f(h)$ takes a uniform distribution, namely $f(h) = 1/\Delta h$. For local sensing, i.e., small Δh, the QFI is almost constant over the interval, and thus $g(\boldsymbol{B}) \approx 1/\mathcal{F}_Q(h^{\mathrm{cen}}|\boldsymbol{B})$. Therefore, the minimization of $g(\boldsymbol{B})$ turns into maximizing $\mathcal{F}_Q(h^{\mathrm{cen}}|\boldsymbol{B})$.

Many-body probe for magnetometry.—To illustrate the relevance of our general formulation for global sensing, which can be applied to any sensing protocol independent of the choice of the probe, we exploit a chain of L interacting spin $-1/2$ particles with an Ising Hamiltonian to sense a random static magnetic field. For simplicity and without loss of generality, we assume that the y component of the magnetic field is zero, as one can always rotate the sample such that $\langle\sigma_y\rangle = 0$. The Hamiltonian is

$$H = J\sum_{i=1}^{L}\sigma_x^i\sigma_x^{i+1} - \sum_{i=1}^{L}[(B_x + h_x)\sigma_x^i + (B_z + h_z)\sigma_z^i], \tag{4}$$

where σ_α^i ($\alpha = x, z$) is the Pauli operator at site i, $J > 0$ is the exchange interaction, $\boldsymbol{B} = (B_x, B_z)$ is the control magnetic field that can be tuned, $\boldsymbol{h} = (h_x, h_z)$ is the random field to estimate, and a periodic boundary condition is imposed. The ground state $|\Phi\rangle$, for which the phase diagram is shown in Fig. 1(a), can be used for detecting the unknown field $\boldsymbol{h}$. See Refs. [82–86] for the link between the characterization of quantum phase transition via metric tensors. The phase diagram is uniquely determined by $(h_z + B_z)/J$ and $(h_x + B_x)/J$. Thus, by tuning $\boldsymbol{B}$ one can shift the phase diagram for the unknown parameter $\boldsymbol{h}$. For example, in the absence of a longitudinal field (i.e., $B_x = h_x = 0$), the ground state $|\Phi\rangle$ can be solved analytically using a Jordan-Wigner transformation and is known to have a quantum phase transition at $h^{\mathrm{crit}} := B_z + h_z = \pm J$ [87,88], which leads to an enhanced QFI with scaling

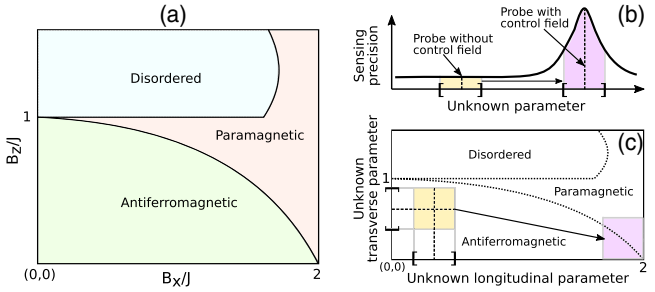

FIG. 1. (a) The phase diagram of an Ising model in the presence of a skew magnetic field (see Ref. [92] for details). (b) By optimizing the control field, the probe is shifted in its phase diagram to operate around the criticality, where the quantum Fisher information is maximum. (c) For multiparameter sensing, the optimization of the probe also displaces the sensing area along the critical line.

$\sim L^2$ [49,51] [see the Supplemental Material [89] (SM) for details]. Interestingly, away from criticality, the QFI scales as $\sim L\xi^{-1}$, where $\xi \sim |(B_z + h_z) - h^{\mathrm{crit}}|^{-1}$ is the correlation length [49]. Since the quantum-enhanced sensing is lost when the probe operates away from criticality, our global sensing formulation stands as the most suitable for these types of sensors.

Example 1: Transverse field Ising probe.—In this section, we use the Ising many-body probe given in Eq. (4) for single-parameter sensing when only a transverse field exists, namely $B_x = h_x = 0$. To see the performance of this probe for global sensing, we numerically evaluate $g(B_z)$ for various Δh for a system size $L = 1000$. In Fig. 2(a), we plot the global sensing performance $g(B_z)$ as a function of B_z/J for different values of interval widths Δh_z and centers h_z^{cen}. For every h_z^{cen} and Δh_z, the average uncertainty $g(B_z)$ always has a minimum that takes place at a particular $B_z = B_z^*$, showing that one can always make the probe optimal by this choice of the control field. Interestingly, the minimum value of $g(B_z)$ is independent of h_z^{cen} and is only determined by Δh_z. On the other hand, the optimal control field B_z^* is almost independent of Δh_z and only depends on h_z^{cen}, such that $h_z^{\mathrm{cen}} + B_z^* \approx h^{\mathrm{crit}}$. This means that the control field tends to shift the probe in its phase diagram such that the interval of sensing is located almost symmetrically around the critical point. This has been shown schematically in Fig. 1(b). To determine how the average uncertainty scales for the optimal probe, in Fig. 2(b), we plot $g(B_z^*)$ as a function of L for various choices of Δh_z. For small Δh_z, the average uncertainty scales as $g(B_z^*) \sim 1/L^2$, which is expected for local sensing. Remarkably, by increasing Δh_z, the scaling goes toward the standard limit, namely $g(B_z^*) \sim 1/L$. To quantify the transition from quantum-enhanced sensing to the standard limit, we fit $g(B_z^*)$ with a function of the form $aL^{-b} + c$, $c \to 0$. In Fig. 2(c), we plot the fitting coefficients a and b as a function of the width $\Delta h_z/J$. As seen from the figure, when $\Delta h_z \to 0$, one recovers the Heisenberg scaling

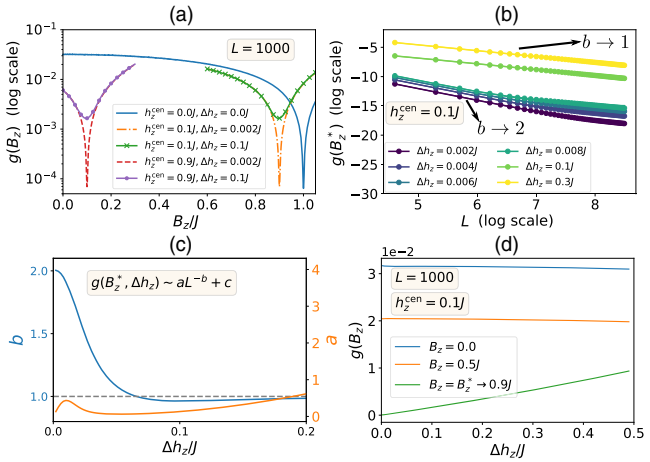

FIG. 2. (a) Average uncertainty $g(B_z)$ as function of B_z/J for different values of interval widths Δh_z and centers h_z^{cen}. The optimal probe can always be found by tuning the control field such that $g(B_z^*) = \min_{B_z}[g(B_z)]$. (b) $g(B_z^*)$ (shown by markers) and its corresponding fitting function $aL^{-b} + c$ (solid lines) as a function of L for various choices of Δh_z. (c) Fitting coefficients a and b versus the controlled field B_z/J. (d) $g(B_z)$ is plotted as a function of $\Delta h_z/J$ for various choices of B_z.

$g(B_z^*) \sim F_Q^{-1} \sim 1/L^2$ from the local sensing strategy. The quantum-enhanced sensing is captured by $b > 1$, for which the precision surpasses the standard limit $b = 1$. Remarkably, the region of quantum-enhanced sensing is extended until $\Delta h_z \leq 0.07$ J, beyond which the standard limit is restored. However, note that the probe's optimization is still beneficial for sensing, even though there is no quantum-enhanced advantage in the scaling. This can be seen in Fig. 2(d), where $g(B_z)$ is plotted as a function of $\Delta h_z/J$ for various choices of B_z. As the figure shows, by the optimal choice of $B_z = B_z^*$, the average uncertainty remains lower than using nonoptimal values of B_z for all Δh_z. In other words, for large Δh_z, while $b = 1$, the a coefficient becomes smaller by optimizing B_z.

Multiparameter global sensing.—Thanks to the above analysis, one can readily generalize the global sensing for the multiparameter case. To set the performance of different multiparameter estimators, we recast the matrix bounds in Eq. (1) into scalar bounds. To do so, we introduce a (positive and real) weight matrix $\mathcal{W}$ such that [74]

$$\mathrm{Tr}[\mathcal{W}\mathrm{Cov}(\boldsymbol{h})] \geq M^{-1}\mathrm{Tr}[\mathcal{F}_Q(\boldsymbol{h}|\boldsymbol{B})^{-1}\mathcal{W}]. \tag{5}$$

The choice of $\mathcal{W}$ depends on the uncertainty that one wants to minimize. Throughout this work, we consider $\mathcal{W}$ to be identity, i.e., $\mathcal{W} = \mathbb{I}$. This choice equally prioritizes the precision of (h_x, h_z) by making the left-hand side of the above inequality to be the sum of the variances of the unknown parameters. Inspired by the single-parameter case, we define the average uncertainty for the multiparameter case as

$$g(\boldsymbol{B}) \coloneqq \int_{\Delta \boldsymbol{h}} f(\boldsymbol{h}) M^{-1} \mathrm{Tr}[\mathcal{F}_Q(\boldsymbol{h}|\boldsymbol{B})^{-1}] d\boldsymbol{h}, \tag{6}$$

where $f(\boldsymbol{h})$ is the prior probability distribution, which is assumed to be uniform, for magnetic field $\boldsymbol{h}$, and the integration is performed over the volume of all parameters. To optimize the probe, one has to minimize $g(\boldsymbol{B})$ with respect to $\boldsymbol{B}$, i.e., $g(\boldsymbol{B}^*) \coloneqq \min_{\boldsymbol{B}}[g(\boldsymbol{B})]$.

Example 2: Skew field Ising probe.—In this section, we consider the probe of Eq. (4), when both h_x and h_z are sensed together. Since the system is not solvable anymore, we are restricted to short chains and exact diagonalization. Unlike the transverse field Ising model for which the criticality happens exactly at one point, here there is a line of criticality in the plane of (h_x, h_z) [92] [see Fig. 1(a)]. Thus, the optimization of the probe is highly nontrivial as the control fields (B_x, B_z) can shift the phase of the probe to operate anywhere along the critical line. For the case of local sensing, in which Δh_x and Δh_z are very small, the minimization of $g(\boldsymbol{B})$ reduces to the maximization of $\mathrm{Tr}\{\mathcal{F}_Q[(h_x^{\mathrm{cen}}, h_z^{\mathrm{cen}})|\boldsymbol{B}]^{-1}\}$.

In contrast to the single-parameter case, our analysis shows that the optimal control fields not only depend on the location of $(h_x^{\mathrm{cen}}, h_z^{\mathrm{cen}})$ but also change by the choice of the widths $(\Delta h_x, \Delta h_z)$. Interestingly, the probe is always shifted somewhere near the critical line, which is predominantly controlled by the longitudinal field. To have a quantitative analysis, in Fig. 3(a) we plot $g(B_x, B_z)$ as a function of control fields for the case of an almost local sensing with $h_x^{\mathrm{cen}} = h_z^{\mathrm{cen}} = 0.02$ J and the widths of $\Delta h_x = \Delta h_z = 0.02$ J. As the figure shows, the optimal control fields are given by $B_x^* = 1.98$ J and $B_z^* = -0.02$ J. In Fig. 3(b), we increase the width to $\Delta h_x = \Delta h_z = 0.3$ J (i.e., global sensing). Interestingly, the optimal control fields shift to $B_x^* = 1.8$ J and $B_z^* = 0.4$ J, which are different from the previous case. This shows that the optimization of the probe for multiparameter sensing is nontrivial and that the optimal control fields depend on the sensing range. This is schematically explained in Fig. 1(c).

Sensing protocol.—While our formulation for global sensing systematically provides a bound for the average uncertainty, it is not obvious whether this bound can be saturated, as no measurement basis can be optimal throughout the whole region. Here, we choose a simple but not necessarily optimal measurement basis, namely global magnetization $M = \sum_i \sigma_z^i$, which can be measured in ion traps [93] and superconducting quantum devices [94,95]. In fact, global magnetization results in $L+1$ outcomes for which one can compute the classical Fisher information matrix. As an example, we consider a two parameter sensing with $h_x^{\mathrm{cen}} = 0.5$ J, $h_z^{\mathrm{cen}} = 0.7$ J, and $\Delta h_x = \Delta h_z = 0.2$ J. One can optimize the probe of Eq. (4) using the algorithm above, i.e., minimizing $g(B_x, B_z)$, which results in $B_x^* = 1.39$ J and $B_z^* = -0.39$ J. Using this optimal probe, we perform the magnetization measurement and compute $\mathrm{Tr}[\mathcal{F}_C(\boldsymbol{h}|\boldsymbol{B}^*)^{-1}]$ over the whole interval. In Fig. 4(a), we plot $\mathrm{Tr}[\mathcal{F}_C(\boldsymbol{h}|\boldsymbol{B}^*)^{-1}]$ as a function of $(h_x + B_x^*)/J$ and $(h_z + B_z^*)/J$. However, one may argue that the optimal control fields, i.e., B_x^* and B_z^*, have been obtained using $\mathcal{F}_Q$ in Eq. (6), which is inherently optimized for the measurement basis. For a fixed measurement basis such as global magnetization, one may replace $\mathcal{F}_Q$ by $\mathcal{F}_C$ in Eq. (6). Since this measurement is not necessarily optimal, the ultimate precision $g(\boldsymbol{B}^*)$ may not be achieved. Nonetheless, optimizing the probe for our given measurement basis, in general, results in different optimal control parameters $\boldsymbol{B}^{*c} = (B_x^{*c}, B_z^{*c})$. Indeed, for the given measurement, using $\boldsymbol{B}^{*c}$ may result in better precision compared to $\boldsymbol{B}^*$. In Fig. 4(b), we plot $\mathrm{Tr}[\mathcal{F}_C(\boldsymbol{h}|\boldsymbol{B}^{*c})^{-1}]$ as a function of $(h_x + B_x^{*c})/J$ and $(h_z + B_z^{*c})/J$. As the figure shows, over the region of interest, the probe optimized by $\mathcal{F}_C$ gives

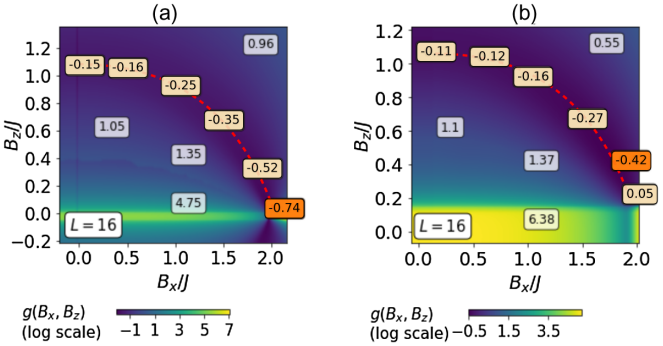

FIG. 3. (a) $g(B_x, B_z)$ as a function of control fields (B_x, B_z) for the case of an almost local sensing $\Delta h_x = \Delta h_z = 0.02$ J. (b) By increasing the widths to $\Delta h_x = \Delta h_z = 0.3$ J, one finds a nontrivial optimal probe along its critical line. The total system is $L = 16$, and centers are chosen to be $h_x^{\mathrm{cen}} = h_z^{\mathrm{cen}} = 0.02$ J. The dashed red lines represent the critical line, and the numbers show the value of $g(B_x, B_z)$ at that point in the phase diagram. The global minimum is depicted in orange.

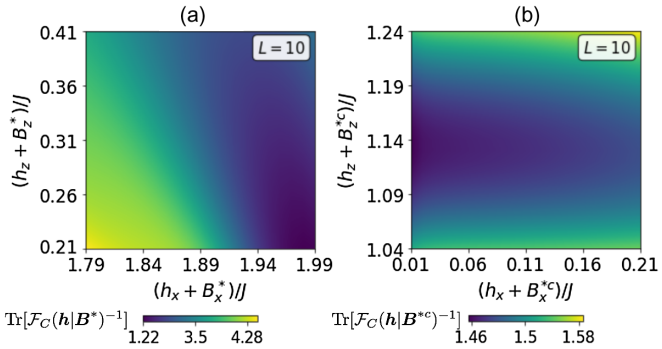

FIG. 4. (a) $\mathrm{Tr}[\mathcal{F}_C(\boldsymbol{h}|\boldsymbol{B}^*)^{-1}]$ as a function of $(h_x + B_x^*)/J$ and $(h_z + B_z^*)/J$. (b) $\mathrm{Tr}[\mathcal{F}_C(\boldsymbol{h}|\boldsymbol{B}^{*c})^{-1}]$ as a function of $(h_x + B_x^{*c})/J$ and $(h_z + B_z^{*c})/J$. The probe optimized with control field $\boldsymbol{B}^{*c}$ provides smaller uncertainty. Other values are $L = 10$, $h_x^{\mathrm{cen}} = 0.5$ J, $h_z^{\mathrm{cen}} = 0.7$ J, $\Delta h_x = \Delta h_z = 0.2$ J, $B_x^* = 1.39$ J, $B_z^* = -0.39$ J, $B_x^{*c} = -0.39$ J, and $B_z^{*c} = 0.44$ J.

smaller uncertainty in contrast to the case shown in Fig. 4(a). Note that both of these still give larger uncertainty than the ultimate bound $g(\boldsymbol{B}^*)$. It is worth emphasizing that B^{*c} and B^* are different due to the presence of the critical line. In the single-parameter case, where the criticality is a single point, B^{*c} coincides with B^* (see the SM for details).

Conclusions.—We present a formulation for multiparameter global sensing that not only provides a bound for the average uncertainty but also allows for systematic optimization of the probe. By applying our protocol to an Ising many-body probe, we show that one can indeed tune external control fields to harness the criticality for enhancing the sensing precision, even when the intervals of interests are so large that the Heisenberg limit is absent. While the optimal measurement basis remains an open problem, we show that a simple magnetization measurement can hugely benefit from our optimization.

This work is supported by the National Key R&D program of China (Grant No. 2018YFA0306703) and National Science Foundation of China (Grants No. 12050410253, No. 92065115, and No. 12050410251). U. M. acknowledges funding from the Chinese Postdoctoral Science Fund for Grant No. 2018M643437. V. M. thanks the Chinese Postdoctoral Science Fund for Grant No. 2018M643435.

*Corresponding author.
vmontenegro@uestc.edu.cn
†Corresponding author.
utkarsh.mishra@uestc.edu.cn
‡Corresponding author.
abolfazl.bayat@uestc.edu.cn

[1] C. L. Degen, F. Reinhard, and P. Cappellaro, Rev. Mod. Phys. **89**, 035002 (2017).
[2] D. Braun, G. Adesso, F. Benatti, R. Floreanini, U. Marzolino, M. W. Mitchell, and S. Pirandola, Rev. Mod. Phys. **90**, 035006 (2018).
[3] G. Tóth and I. Apellaniz, J. Phys. A **47**, 424006 (2014).
[4] V. Giovannetti, S. Lloyd, and L. Maccone, Nat. Photonics **5**, 222 (2011).
[5] F. Albarelli, M. A. C. Rossi, M. G. A. Paris, and M. G. Genoni, New J. Phys. **19**, 123011 (2017).
[6] V. Giovannetti, S. Lloyd, and L. Maccone, Nature (London) **412**, 417 (2001).
[7] A. N. Boto, P. Kok, D. S. Abrams, S. L. Braunstein, C. P. Williams, and J. P. Dowling, Phys. Rev. Lett. **85**, 2733 (2000).
[8] D. Leibfried, M. D. Barrett, T. Schaetz, J. Britton, J. Chiaverini, W. M. Itano, J. D. Jost, C. Langer, and D. J. Wineland, Science **304**, 1476 (2004).
[9] V. Giovannetti, S. Lloyd, and L. Maccone, Phys. Rev. Lett. **96**, 010401 (2006).
[10] V. Giovannetti, S. Lloyd, and L. Maccone, Science **306**, 1330 (2004).
[11] F. Belliardo and V. Giovannetti, Phys. Rev. A **102**, 042613 (2020).
[12] S. M. Roy and S. L. Braunstein, Phys. Rev. Lett. **100**, 220501 (2008).
[13] S. Boixo, S. T. Flammia, C. M. Caves, and J. M. Geremia, Phys. Rev. Lett. **98**, 090401 (2007).
[14] A. De Pasquale, D. Rossini, P. Facchi, and V. Giovannetti, Phys. Rev. A **88**, 052117 (2013).
[15] M. Skotiniotis, P. Sekatski, and W. Dr, New J. Phys. **17**, 073032 (2015).
[16] S. Pang and T. A. Brun, Phys. Rev. A **90**, 022117 (2014).
[17] F. Albarelli, M. A. C. Rossi, D. Tamascelli, and M. G. Genoni, Quantum **2**, 110 (2018).
[18] W. Dür and H.-J. Briegel, Phys. Rev. Lett. **92**, 180403 (2004).
[19] R. Demkowicz-Dobrzański, J. Kołodyński, and M. GuŢă, Nat. Commun. **3**, 1063 (2012).
[20] Y. Matsuzaki, S. C. Benjamin, and J. Fitzsimons, Phys. Rev. A **84**, 012103 (2011).
[21] A. Shaji and C. M. Caves, Phys. Rev. A **76**, 032111 (2007).
[22] S. F. Huelga, C. Macchiavello, T. Pellizzari, A. K. Ekert, M. B. Plenio, and J. I. Cirac, Phys. Rev. Lett. **79**, 3865 (1997).
[23] J. Cai, F. Caruso, and M. B. Plenio, Phys. Rev. A **85**, 040304 (R) (2012).
[24] J. Liu and H. Yuan, Phys. Rev. A **96**, 012117 (2017).
[25] J. Liu and H. Yuan, Phys. Rev. A **96**, 042114 (2017).
[26] P. Sekatski, M. Skotiniotis, J. Kołodyński, and W. Dür, Quantum **1**, 27 (2017).
[27] A. Hentschel and B. C. Sanders, Phys. Rev. Lett. **107**, 233601 (2011).
[28] H. Xu, J. Li, L. Liu, Y. Wang, H. Yuan, and X. Wang, npj Quantum Inf. **5**, 82 (2019).
[29] V. Cimini, I. Gianani, N. Spagnolo, F. Leccese, F. Sciarrino, and M. Barbieri, Phys. Rev. Lett. **123**, 230502 (2019).
[30] J. J. Meyer, J. Borregaard, and J. Eisert, arXiv:2006.06303.
[31] N. B. Lovett, C. Crosnier, M. Perarnau-Llobet, and B. C. Sanders, Phys. Rev. Lett. **110**, 220501 (2013).
[32] H. Yuan and C.-H. F. Fung, Phys. Rev. Lett. **115**, 110401 (2015).
[33] S. Pang and A. N. Jordan, Nat. Commun. **8**, 14695 (2017).
[34] M. Naghiloo, A. N. Jordan, and K. W. Murch, Phys. Rev. Lett. **119**, 180801 (2017).
[35] L. J. Fiderer and D. Braun, Nat. Commun. **9**, 1351 (2018).
[36] J. E. Lang, R. B. Liu, and T. S. Monteiro, Phys. Rev. X **5**, 041016 (2015).
[37] U. Mishra and A. Bayat, arXiv:2010.09050.
[38] C. Bonato, M. S. Blok, H. T. Dinani, D. W. Berry, M. L. Markham, D. J. Twitchen, and R. Hanson, Nat. Nanotechnol. **11**, 247 (2016).
[39] B. L. Higgins, D. W. Berry, S. D. Bartlett, H. M. Wiseman, and G. J. Pryde, Nature (London) **450**, 393 (2007).
[40] D. W. Berry, B. L. Higgins, S. D. Bartlett, M. W. Mitchell, G. J. Pryde, and H. M. Wiseman, Phys. Rev. A **80**, 052114 (2009).
[41] G. S. Jones, S. Bose, and A. Bayat, arXiv:2003.02308.
[42] M. Beau and A. del Campo, Phys. Rev. Lett. **119**, 010403 (2017).
[43] L.-S. Guo, B.-M. Xu, J. Zou, and B. Shao, Sci. Rep. **6**, 33254 (2016).
[44] A. M. Rey, L. Jiang, and M. D. Lukin, Phys. Rev. A **76**, 053617 (2007).

[45] S. Choi and B. Sundaram, Phys. Rev. A **77**, 053613 (2008).
[46] S. Boixo, A. Datta, M. J. Davis, S. T. Flammia, A. Shaji, and C. M. Caves, Phys. Rev. Lett. **101**, 040403 (2008).
[47] S. Boixo, A. Datta, M. J. Davis, A. Shaji, A. B. Tacla, and C. M. Caves, Phys. Rev. A **80**, 032103 (2009).
[48] J. Czajkowski, K. Pawłowski, and R. Demkowicz-Dobrzański, New J. Phys. **21**, 053031 (2019).
[49] M. M. Rams, P. Sierant, O. Dutta, P. Horodecki, and J. Zakrzewski, Phys. Rev. X **8**, 021022 (2018).
[50] C. Invernizzi, M. Korbman, L. C. Venuti, and M. G. A. Paris, Phys. Rev. A **78**, 042106 (2008).
[51] P. Zanardi, M. G. A. Paris, and L. Campos Venuti, Phys. Rev. A **78**, 042105 (2008).
[52] S. Gammelmark and K. Mølmer, New J. Phys. **13**, 053035 (2011).
[53] G. Salvatori, A. Mandarino, and M. G. A. Paris, Phys. Rev. A **90**, 022111 (2014).
[54] M. Bina, I. Amelio, and M. G. A. Paris, Phys. Rev. E **93**, 052118 (2016).
[55] I. Frérot and T. Roscilde, Phys. Rev. Lett. **121**, 020402 (2018).
[56] Y. Chu, S. Zhang, B. Yu, and J. Cai, Phys. Rev. Lett. **126**, 010502 (2021).
[57] L. Garbe, M. Bina, A. Keller, M. G. A. Paris, and S. Felicetti, Phys. Rev. Lett. **124**, 120504 (2020).
[58] M. A. C. Rossi, M. Bina, M. G. A. Paris, M. G. Genoni, G. Adesso, and T. Tufarelli, Quantum Sci. Technol. **2**, 01LT01 (2017).
[59] M. Mehboudi, L. A. Correa, and A. Sanpera, Phys. Rev. A **94**, 042121 (2016).
[60] R. Okamoto, M. Iefuji, S. Oyama, K. Yamagata, H. Imai, A. Fujiwara, and S. Takeuchi, Phys. Rev. Lett. **109**, 130404 (2012).
[61] R. Okamoto, S. Oyama, K. Yamagata, A. Fujiwara, and S. Takeuchi, Phys. Rev. A **96**, 022124 (2017).
[62] A. Fujiwara, J. Phys. A **39**, 12489 (2006).
[63] A. Fujiwara, J. Phys. A **44**, 079501 (2011).
[64] H. M. Wiseman, Phys. Rev. Lett. **75**, 4587 (1995).
[65] B. L. Higgins, D. W. Berry, S. D. Bartlett, H. M. Wiseman, and G. J. Pryde, Nature (London) **450**, 393 (2007).
[66] M. A. Armen, J. K. Au, J. K. Stockton, A. C. Doherty, and H. Mabuchi, Phys. Rev. Lett. **89**, 133602 (2002).
[67] W.-K. Mok, K. Bharti, L.-C. Kwek, and A. Bayat, arXiv: 2010.14200.
[68] J. Rubio, J. Anders, and L. A. Correa, arXiv:2011.13018.
[69] H. Cramer, *Mathematical Methods of Statistics* (Princeton University Press, Princeton, 1946).
[70] S. L. Braunstein and C. M. Caves, Phys. Rev. Lett. **72**, 3439 (1994).
[71] M. G. A. Paris, Int. J. Quantum. Inform. **07**, 125 (2009).
[72] J. Liu, H. Yuan, X.-M. Lu, and X. Wang, J. Phys. A **53**, 023001 (2020).
[73] L. Seveso and M. G. A. Paris, Int. J. Quantum. Inform. **18**, 2030001 (2020).
[74] F. Albarelli, M. Barbieri, M. Genoni, and I. Gianani, Phys. Lett. A **384**, 126311 (2020).
[75] L. M. Le Cam, *Asymptotic Methods in Statistical Decision Theory*, Springer Series in Statistics (Springer-Verlag, New York, 1986).
[76] Z. Hradil, R. Myška, J. Peřina, M. Zawisky, Y. Hasegawa, and H. Rauch, Phys. Rev. Lett. **76**, 4295 (1996).
[77] L. Pezzé, A. Smerzi, G. Khoury, J. F. Hodelin, and D. Bouwmeester, Phys. Rev. Lett. **99**, 223602 (2007).
[78] J. Rubio and J. Dunningham, New J. Phys. **21**, 043037 (2019).
[79] S. Olivares and M. G. A. Paris, J. Phys. B **42**, 055506 (2009).
[80] R. Fletcher, Newton-like methods, in *Practical Methods of Optimization* (John Wiley & Sons, Ltd, New York, 2000), Chap. 3, pp. 44–79.
[81] S. Mirjalili, Genetic algorithm, in *Evolutionary Algorithms and Neural Networks: Theory and Applications* (Springer International Publishing, Cham, 2019), pp. 43–55.
[82] L. Campos Venuti and P. Zanardi, Phys. Rev. Lett. **99**, 095701 (2007).
[83] P. Zanardi and N. Paunković, Phys. Rev. E **74**, 031123 (2006).
[84] H.-Q. Zhou, J.-H. Zhao, and B. Li, J. Phys. A **41**, 492002 (2008).
[85] P. Zanardi, P. Giorda, and M. Cozzini, Phys. Rev. Lett. **99**, 100603 (2007).
[86] A. T. Rezakhani, D. F. Abasto, D. A. Lidar, and P. Zanardi, Phys. Rev. A **82**, 012321 (2010).
[87] D. S. Fisher, Phys. Rev. B **51**, 6411 (1995).
[88] S. Sachdev, *Quantum Phase Transitions*, 2nd ed. (Cambridge University Press, Cambridge, England, 2011).
[89] See Supplemental Material, which includes Refs. [90,91], at http://link.aps.org/supplemental/10.1103/PhysRevLett.126.200501 for the analytical solution in obtaining the ground state of the transverse Ising chain and how to evaluate the quantum Fisher information for this case.
[90] A. Dutta, G. Aeppli, B. K. Chakrabarti, U. Divakaran, T. F. Rosenbaum, and D. Sen, *Quantum Phase Transitions in Transverse Field Spin Models: From Statistical Physics to Quantum Information* (Cambridge University Press, Cambridge, England, 2015).
[91] B. Damski and M. M. Rams, J. Phys. A **47**, 025303 (2014).
[92] O. F. de Alcantara Bonfim, B. Boechat, and J. Florencio, Phys. Rev. E **99**, 012122 (2019).
[93] C. Kokail, C. Maier, R. van Bijnen, T. Brydges, M. K. Joshi, P. Jurcevic, C. A. Muschik, P. Silvi, R. Blatt, C. F. Roos, and P. Zoller, Nature (London) **569**, 355 (2019).
[94] B. Chiaro, C. Neill, A. Bohrdt, M. Filippone, F. Arute, K. Arya, R. Babbush, D. Bacon, J. Bardin, R. Barends, S. Boixo *et al.*, arXiv:1910.06024.
[95] F. Arute, K. Arya, R. Babbush, D. Bacon, J. C. Bardin, R. Barends, R. Biswas, S. Boixo, F. G. S. L. Brandao, D. A. Buell, B. Burkett *et al.*, Nature (London) **574**, 505 (2019).